

Fault diagnosis of gearbox in wind turbine based on EMD-DCGAN

Guangyi Meng^{1,*}, Yuxing An¹, Dong Zhang¹ and Xudong Li¹

¹Shenyang Institute of Engineering, Shenyang 110136, Liaoning, China

Abstract

INTRODUCTION: Wind turbine gearbox fault diagnosis is of great significance for the safe and stable operation of wind turbines. The accuracy of wind turbine gearbox fault diagnosis can be effectively improved by using complete wind turbine gearbox fault data and efficient fault diagnosis algorithms. A wind turbine gearbox fault diagnosis method based on EMD-DCGAN method is proposed in this paper.

OBJECTIVES: It can solve the problem when the sensor fails or the data transmission fails, it will lead to errors in the wind turbine gearbox fault data, which in turn will lead to a decrease in the wind turbine gearbox fault diagnosis accuracy.

METHODS: Firstly, the outliers in the sample data need to be detected and removed. In this paper, the EMD method is used to eliminate outliers in the wind turbine gearbox fault data samples with the aim of enhancing the true continuity of the samples; secondly, in order to make up for the lack of missing samples, a data enhancement algorithm based on a GAN network is proposed in the paper, which is able to effectively perfect the missing items of the sample data; lastly, in order to improve the accuracy of wind turbine gearbox faults, a DCGAN neural network-based fault diagnosis method is proposed, which effectively combines the data dimensionality reduction feature of deep learning method and the data enhancement feature of generative adversarial network, and can improve the accuracy and speed of fault diagnosis.

RESULTS and CONCLUSIONS: The experimental results show that the proposed method can effectively identify wind turbine gearbox fault conditions, and verify the effectiveness of the algorithm under different sample data conditions.

Keywords: Empirical mode decomposition method; Data expansion; Generative adversarial neural network; Fault diagnosis of wind turbine gearbox

Received on 23 December 2023, accepted on 29 March 2024, published on 05 April 2024

Copyright © 2024 G. Meng *et al.*, licensed to EAI. This is an open access article distributed under the terms of the [CC BY-NC-SA 4.0](https://creativecommons.org/licenses/by-nc-sa/4.0/), which permits copying, redistributing, remixing, transformation, and building upon the material in any medium so long as the original work is properly cited.

doi: 10.4108/ew.5652

1. Introduction

Wind turbines have developed considerably with the increasing global energy problems and the development of new technologies. In 2019, the newly installed capacity reached a record high. The newly-added wind turbine assembly capacity is 60.04GW, and the cumulative installed capacity is 658.41GW^[1-4]. As shown in Figure 1, one year later, the cumulative global installed capacity in 2020 will increase to 721.64GW, and the global new installed capacity is likely to increase to 78GW in 2021. In 2018, the newly integrated wind energy into the National Grid was

2.03×107kW, and the cumulative amount was 1.84×108kW^[5-8]. The annual wind power utilization time was 2,103 hours, an increase of 153 hours over the previous year, and the newly installed capacity remained at about 2.0×107kW/year.

*Corresponding author. Email: menggy@sie.edu.cn

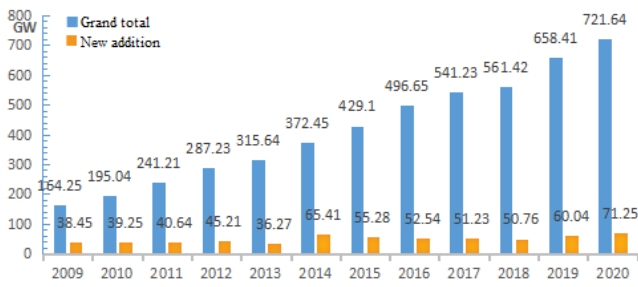


Figure 1. The number of new machines installed and the cumulative number of wind turbines installed

As a power generation equipment, wind turbines are subject to significantly higher operation and maintenance costs due to the production process materials and the operating environment, and random failures may occur in various components. In particular, there are numerous coupling links in the wind turbine gearbox, and it has a very high probability of failure. Although the service life of a wind turbine is typically 20 years, the wind turbine gearbox will fail many times during the entire life cycle of the wind turbine. However, because of long-term working in complex environments such as gobi, plateau, seaside, etc, it is difficult for wind turbines to reach the service life. In many places, wind turbines appear kinds of failure more than 5 years after being put into production^[9-14]. The gearbox has a core role. Due to its many components and large installation losses, the gearbox has become a concentrated location for failures. Whether the gearbox is normal or not directly affects the normal operation of the wind turbine.

At present, wind turbine gearbox fault diagnosis has been carried out by many research institutions and scholars for a large number of studies. Generally speaking, the research of wind turbine gearbox fault diagnosis is to monitor some characteristic parameters such as thermal imaging parameters and vibration parameters during the operation of wind turbine gearbox, use the relevant parameters to train the diagnostic model, get the deviation between the current state and the normal state, and use the judgement of the deviation to achieve the wind turbine gearbox fault diagnosis. The intelligent algorithms used in the wind turbine gearbox fault diagnosis model mainly include traditional intelligent algorithms and deep learning algorithms. The research team from Henan University of Science and Technology used

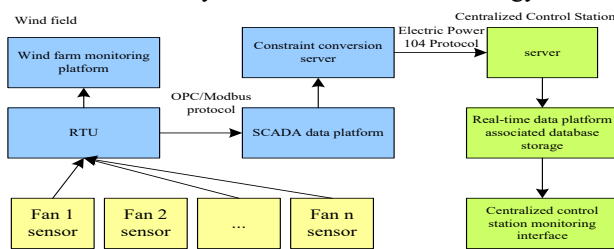


Figure 2. Data transmission mode between the wind farm SCADA system and the centralized control station

fewer sample data for wind turbine gearbox fault diagnosis and utilised the least squares support vector machine method to achieve wind turbine gearbox faults, and the results show that the proposed method can effectively improve the speed of diagnosis. There are many fault diagnosis methods for wind turbines^[15-20]. In the wind turbine gearbox fault diagnosis method, the accurate selection of fault features is the key to establish an efficient fault diagnosis method. In the process of fault feature selection, the use of cost function to evaluate the features can effectively evaluate the correlation between multidimensional features, which has a better effect on fault feature selection. However, it is difficult to accurately characterise all the faults in wind turbine gearbox fault diagnosis by a single application of the cost function. Moreover, the vibration signals of wind turbine gearbox fault diagnosis will be affected by the sensors and thus have trend terms, which will further adversely affect the results of wind turbine gearbox fault diagnosis.

In summary, this paper proposes a fault diagnosis method for wind turbine gearbox based on EMD-DCGAN. First, in view of the fault error of the wind turbine gearbox, the empirical mode analysis method (EMD) is used to eliminate the trend item of the vibration sample waveform of the fault data, and the authenticity of the fault sample is improved; Database data expansion sample; then, use deep convolutional generative confrontation neural network (DCGAN) to diagnose fault vibration data; finally, use historical data and enhanced data to verify DCGAN, and prove that GAN uses EMD processed data Expand the training samples to improve the accuracy of DCGAN wind turbine gearbox fault diagnosis.

2. Analysis of wind turbine gearbox fault diagnosis mechanism

The SCADA system has been widely used in wind turbines to detect and record operating parameters. The system generally stores and records all the operating data of the wind turbines every five minutes. As shown in Figure 2, these data are basically installed The sensor inside the wind turbine collects and uploads. These numerous SCADA data contain a large amount of wind turbine operation information, which can be used to analyze the operation status and fault diagnosis of wind turbines by using appropriate analysis methods or algorithms.

The control system needs to monitor multiple subsystems, the operating state parameters and environmental parameters of various parts of the main wind turbine. When the measured value of a parameter related to the operating status of the entire unit exceeds the safety threshold, an instruction will be issued to order the unit to stop. If it is not an emergency fault or just reaches the critical value of the safety threshold, only an alarm will be issued without shutting down. When the unit fails or alarms, the system will write the time and specific information of the failure into the operation report and store it in the database. The table 1 shows the operating state parameters and environmental

parameters of various parts of the wind turbine during operation.

Table 1. Operating state parameters of various parts of the wind turbine

Wheel speed	Blade angle	Wind speed	Absolute wind direction	Bearing temperature	temperat ure	Minimum gearbox vibration frequency	Maximum gearbox vibration frequency
1.53	30.93	2.26	128.85	10.2	14.9	0	-0.24
6.15	3.32	2.41	98.492	12.7	15	0	-0.27
2.54	54.53	2.01	103.78	16.5	15	0	-0.29
0.37	63.14	2.72	113.94	15.9	14.9	-0.05	-0.21
5.44	6.44	3.08	126.57	16.8	14.5	0	-0.27
7.27	0.5	3.68	119.84	20.5	14.2	0	-0.24
7.28	0.5	3.57	114.24	23.5	13.9	-0.04	-0.23
7.44	0.5	4.31	111.43	26	13.6	-0.05	-0.25
7.59	0.5	4.37	104.96	28.1	13.1	-0.05	-0.21
8.75	0.5	5.39	104.50	30.2	12.8	-0.03	-0.22
8.73	0.5	5.12	101.16	32.3	12.4	-0.07	-0.23
8.16	0.49	4.73	104.94	33.9	12.1	0	-0.21
9.17	0.49	5.38	99.99	35.2	11.9	0	-0.21
9.25	0.5	5.35	100.85	37	12.2	-0.08	-0.2
9.61	0.5	5.73	109.78	38.1	12.3	-0.03	-0.22
8.85	0.5	5.24	112.68	39.2	12.5	-0.04	-0.24
10.65	0.5	6.41	113.86	40.2	12.4	-0.05	-0.23
10.5	0.5	6.25	118.59	41.7	12.5	-0.05	-0.22
10.46	0.5	6.38	109.12	42.6	12.5	0	-0.22
9.94	0.49	6.06	109.92	43.4	12.4	0	-0.24
9.7	0.5	5.83	111.92	44	12.4	-0.04	-0.24
...
10.29	0.5	5.9	107.64	44.7	12.6	-0.06	-0.22
10.31	0.49	6.4	116.94	45.2	12.6	0	-0.22
10.57	0.5	6.56	109.64	45.9	12.6	-0.05	-0.21

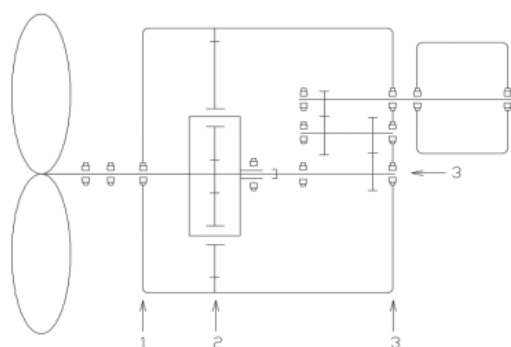


Figure 3. The location of the gearbox vibration measurement point

According to the characteristics of the wind turbine model, as shown in Figure 3, the gearbox vibration detection data has four detection points 1234 along the transmission direction, and each position is tested for the horizontal and

vertical speed waveforms and frequencies, as well as acceleration waveforms and frequencies. In addition, the acceleration demodulation spectrum detection item is added to the detection position on No. 2 and later to facilitate the analysis of the gear teeth and bearing status, as shown in Table 2.

Table 2 Various parameters monitored by the observation points on the gearbox

Location number	Measuring point number	Location name	Testing direction	Contents of detection
I_1	a	Gearbox input	Horizontal	Gearbox vibration frequency/vibration wave type
	b	Gearbox input	Vertical	Gearbox vibration frequency/vibration wave type
I_2	a	Gearbox low speed shaft output end	Horizontal	Gearbox vibration frequency/vibration wave type
	b	Gearbox low speed shaft output end	Vertical	Gearbox vibration frequency/vibration wave type
I_3	a	Gearbox high speed shaft output end	Horizontal	Gearbox vibration frequency/vibration wave type
	b	Gearbox high speed shaft output end	Vertical	Gearbox vibration frequency/vibration wave type
I_4	a	Planetary end of gearbox	Horizontal	Gearbox vibration frequency/vibration wave type
	b	Planetary end of gearbox	Vertical	Gearbox vibration frequency/vibration wave type

Vibration signals can characterise the operating status of wind turbines, and therefore, they play a crucial role in the fault diagnosis of wind turbine gearboxes. Assuming that the rated rotational speed of the wind turbine is 2,900 rpm and the frequency is $2,900/60=48.33$ Hz, and that the wind turbine rolling bearing adopts the traditional structure, which consists of the outer ring, the inner ring, the cage, and the rolling body, the formula for calculating the characteristic frequency of the key components of the wind turbine rolling bearing is as follows:

$$f_1 = \frac{r}{60} \frac{1}{2} N \left(1 - \frac{d}{D} \cos \alpha\right) \quad (1)$$

$$f_2 = \frac{r}{60} \frac{1}{2} N \left(1 + \frac{d}{D} \cos \alpha\right) \quad (2)$$

$$f_3 = \frac{r}{60} \frac{1}{2} \left(1 - \frac{d}{D} \cos \alpha\right) \quad (3)$$

$$f_4 = \frac{r}{60} \frac{1}{2} \frac{D}{d} \left(1 - \left(\frac{d}{D}\right)^2 \cos^2 \alpha\right) \quad (4)$$

3. Empirical Mode Decomposition (EMD) fault data processing and deep convolutional generative countermeasure network (DCGAN) fault diagnosis model

3.1. Principles of Generative Adversarial Network (GAN)

Generative Adversarial Network needs to train the network using input data z and real samples x . At the same time, the generator is used to output the result $G(z)$, and the discriminator is used to output $D(x)$ and $D(G(z))$ results respectively. If the sample data meets the pre-conditions, then the discriminator outputs the wanted state as $D(x)=1$. $D(G(z))=0$. The GAN network can be optimised using the discriminator outputs as well as the network parameters to build the optimisation model as follows:

$$\min_G \max_D J(D, G) = E_{x \sim P_{data}} \log D(x) + E_{z \sim p_z(z)} \log(1 - D(G(z))) \quad (5)$$

where: $V(D,G)$ represents the overall objective function of the generated confrontation network, $\min V(D,G)$ represents the objective function of the generator, and $\max V(D,G)$ represents the objective function of the discriminator. $z \sim p(z)$ indicates that z conforms to the coded statistical $p(z)$, that is, z is a random number sampled from the coded statistical distribution^[14-16].

Generative Adversarial Networks are characterised by the use of alternating training of the generator and the discriminator thus enabling the optimisation process of the final network. Specifically, the parameters of the generator and discriminator are updated alternately and iteratively, and

there is no simultaneous parameter update. In the early stage of network training, the generator is significantly weaker than the discriminator due to its generative effect, therefore, at this time, the discriminator will not be updated with parameters, and only the generator G network parameters will be updated, and after the update iteration, in order to get a better generative adversarial network, the parameters of the discriminator D network need to be updated, and ultimately, under iterative updating of the generator network and the discriminator network, we get the maximum value of (D, G) condition of the optimal objective function V . The specific workflow is shown in Figure 4:

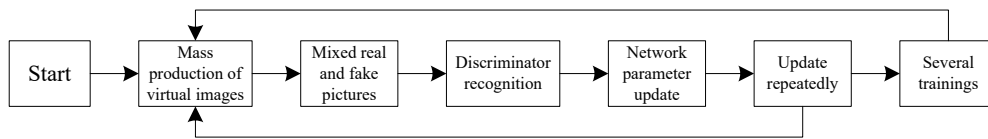


Figure 4. Train of Thoughts on Sample Training of Generative Adversarial Neural Network

3.2 Empirical Mode Decomposition (EMD) processing fault data

EMD has a better effect on signal smoothing, which is due to the fact that EMD uses the fluctuation characteristics and trend characteristics of signals of different time scales to process non-smooth signals, which can reflect the characteristics of signals at different frequencies, and the characteristics can better reflect the real pattern of the original signals.^[17]. Each band of the signal sequence has a mode function corresponding to it, and each IMF has specific conditions:

- (1) IMF should contain at least two extreme values, reflecting the maximum and minimum ranges of IMF. And there are strict requirements on the number of IMF poles, i.e., the number of poles is the same as or differs from the number of over-zero points by one.
- (2) If the local maximum of the signal is defined as the upper envelope and the local minimum of the signal is defined as the lower envelope, then the average of the upper and lower envelopes computed for each time point on the time scale should be zero as well.

EMD, the signal processing mechanism on this time scale, is defined as a filtering process for the data. Assuming that the original signal is $x(t)$, the signal processing process based on EMD according to the EMD processing signal mechanism is as follows:

- a) Use the original signal as the input to the EMD to obtain the maximum value of the original signal.;
- b) Fitting to the maximum value, the maximum and minimum values of the original signal are fitted by the cubic spline interpolation function. If the local maximum value of the signal is defined as the upper envelope $e_+(t)$ and the local minimum value of the signal is defined as

the lower envelope $e_-(t)$, the average value obtained by using the upper and lower envelopes is defined as $m_1(t)$:

$$m_1(t) = (e_+(t) + e_-(t)) \div 2 \quad (6)$$

c) According to the EMD processing signal mechanism, the difference values affected by the original signal $x(t)$ and the average value $m_1(t)$ are calculated to obtain the difference function $z_{1.1}(t)$ as follows:

$$z_{1.1}(t) = x(t) - m_1(t) \quad (7)$$

The original signal $x(t)$ can be represented by the IMF component as

$$x(t) = \sum_{i=1}^n c_i(t) + r_n(t) \quad (8)$$

According to the EMD processing signal mechanism, it can be seen that the decomposition strategy is to decompose the original signal at different frequencies, and the final decomposed signal includes fixed modal components and residuals, which are equivalent to the original signal. Different natural modal components contain different frequency components, and as the order of IMF increases, the frequency components contained in them gradually decrease, and the lowest frequency component is $r_n(t)$. The first few IMF components obtained by empirical mode decomposition usually contain most of the information of the original signal^[18-20]. Combined with the long period of the trend term, that is, the characteristics of low frequency, the first few IMF components are summed to obtain an approximate signal of the original signal. This approximation The signal is the useful signal after removing the trend item.

3.3 Enhanced model for wind turbine gearbox fault diagnosis sample data based on DCGAN neural network

Convolutional neural networks are good at dealing with multidimensional nonlinear feature data, this is due to the fact that convolutional neural networks contain convolutional and pooling layers, which can achieve the extraction of data features from the network structure perspective. The convolutional layer serves as a key link in the convolutional neural network, but has special structural characteristics, so the convolutional layer is sparsely connected to other layers.

(1) Convolution surface calculation

The convolutional layer generally has multiple convolution kernels, mainly for extracting deeper features, so the parameters of the convolution kernel are emphasized during network training. The input matrix of the convolutional layer is defined as x and the matrix has M rows and N columns, then the size of the convolutional kernel is also the same as the input matrix, the convolutional kernel is defined as w , and the bias in the convolutional network is defined as b . The convolutional layer is calculated as:

$$h = x \tilde{*} w + b \quad (9)$$

If each channel is input, there are D matrices x_1, x_2, \dots, x_D , and the corresponding convolution kernels are w_1, w_2, \dots, w_D , and the offset is b , which means that the formula is:

$$h = \sum_{i=1}^D x_i \tilde{*} w_i + b \quad (10)$$

(2) Partial response normalization

The value on the convolution surface is defined as y and the local response as bix , then the normalised value of y is calculated as follows:

$$b_{x,y}^i = a_{x,y}^i / (k + \alpha \sum_{j=\max(0, i-n/2)}^{\min(N-1, i+n/2)} (a_{x,y}^j)^2)^\beta \quad (11)$$

where n is the number of neighbouring convolutional surfaces in the convolutional layer, k , α and β are tunable parameters in the convolutional layer which can be adjusted according to the data characteristics, and N is the total number of convolutional surfaces. Since the local response has been normalised, the convolutional network needs to be re-tuned for the corresponding parameters. The expression of the objective function E is:

$$\frac{\partial b_{x,y}^j}{\partial a_{x,y}^i} \begin{cases} M_i^{-\beta} - (2\alpha\beta) \bullet a_{x,y}^i \bullet b_{x,y}^j \bullet M_i^{-1}, j = i \\ -2\alpha\beta a_{x,y}^i b_{x,y}^j M_i^{-1}, j \neq i \end{cases} \quad (12)$$

4. Example simulation

The convolutional neural network used in the wind turbine gearbox fault diagnosis model in this paper consists of an input layer, a convolutional layer, a pooling layer, and a convolutional residual module, in which the convolutional layer is denoted by conv1 with the number of 4, the maximum pooling layer is denoted by maxpool with the number of 4, and the convolutional residual module is denoted by onv2_x, conv3_x, conv4_x and conv5_x. with the number 4. Firstly the vibration signal data is input, for the first convolutional layer the amount of convolutional kernels in the layer is set to 16, the size of the convolutional kernel is preferred to be 3 x 3 according to the vibration signal data and the step size is 1. The training parameters are set to 448 accordingly. The pooling layer step size is 2x2 and 1. For the second convolutional layer the number of convolutional kernels is set to 32, the convolutional kernel size is preferred to be 3 x 3 based on the vibration signal data and the step size is 1. The training parameters are set to 4640 accordingly. The pooling layer step size is 2x2 and 1. For the third convolutional layer the number of convolutional kernels is set to 64, the size of the convolutional kernel is preferred to be 3 x 3 based on the vibration signal data, and the step size is 1. The training parameters are set to 18,496 accordingly. The pooling layer has a step size of 2x2 and a step size of 1. For the fourth convolutional layer the number of convolutional kernels is set to 128, the convolutional kernel size is preferred to be 3 x 3 based on the vibration signal data and the step size is 1. The training parameters are set to 73,856 accordingly. The pooling layer step size is 2x2 and 1. For the fully connected layer in the wind turbine gearbox fault diagnosis model, the activation function needs to be selected, and in this paper, the relu function is selected as the activation parameter. The number of convolutions in the fully connected layer is set to 100, and the training parameters are set to 43 059 300 accordingly. The relu function is selected as the activation function of the second fully connected layer. The number of convolutions in the second fully connected layer is set to 10, and the training parameters are set to 43 059 300 accordingly. The softmax function was chosen as the activation function for the second fully connected layer. The number of convolutions in the third fully connected layer is set to 2 and the training parameters are set to 202 accordingly.

4.1 EMD eliminates data trend items

In order to verify the feasibility and efficiency of the empirical mode decomposition method for optimizing fault vibration data, this paper selects the fault vibration

waveform diagram prepared in Matlab before the study as the source signal, as shown in Figure 5, observe the wind speed and weather conditions before the vibration detection , Avoid extreme weather operations. During the acquisition process, the wind turbine is started. When the generator speed reaches 1,200 rpm and is relatively stable, the data will be collected. When the acquisition time meets the requirements, it will move to the next acquisition point for vibration data acquisition.

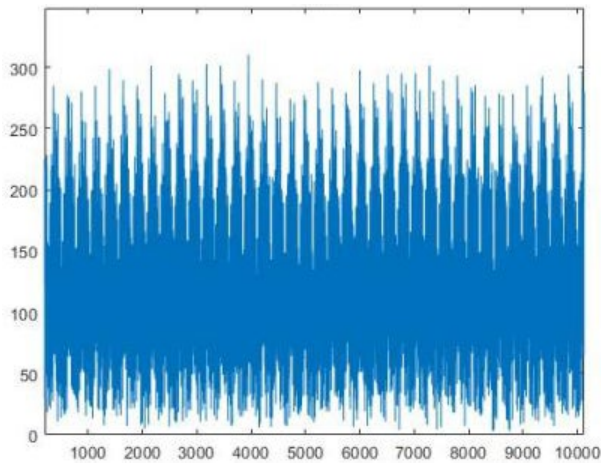


Figure 5. Vibration diagram of wind turbine during normal operation

Vibration signals containing trend items will have a greater impact on the subsequent analysis results, and even deviate far from the normal analysis results. According to the above analysis, using the empirical mode decomposition method to process vibration signals containing trend items can eliminate The influence of the trend item on the analysis result. Common trend items mainly include linear trend items, polynomial trend items and exponential trend items, which are defined as follows:

Linear trend item

$$c(t) = a_0 + a_1t \quad (13)$$

Polynomial trend term

$$c(t) = a_0 + a_1t + a_2t^2 + a_3t^3 + \dots + a_nt^n \quad (14)$$

Index trend item

$$c(t) = ae^{-bt} \quad (15)$$

In order to verify the effectiveness of the empirical modal decomposition method to eliminate the trend item in the vibration signal, the on-site wind turbine equipment vibration data and the trend item generated by the simulation are combined to form the vibration data containing the trend item on the MATLAB platform. Perform processing and compare and analyze the data

before and after processing. Select 5,000 data from the vibration data set of the on-site wind turbine equipment.

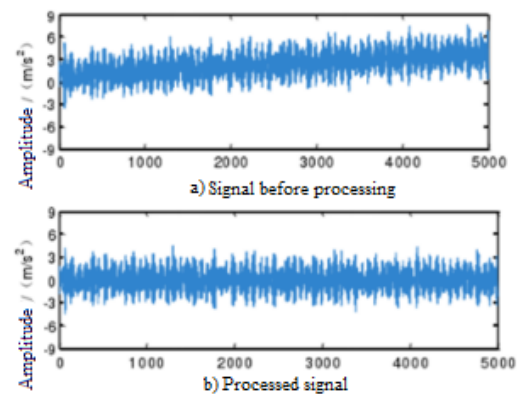


Figure 6. Comparison before and after EMD treatment

As shown in Figure 6, it can be seen from the processed graph that it mainly fluctuates up and down at zero, indicating that these data do not contain trend items. This is mainly because the trend items may only appear after the collection equipment has been working for a long time. The data collection of the experimental platform was completed in a relatively short time, and the preprocessing of the vibration data was completed by using empirical mode decomposition.

4.2 GAN fault virtual data generation

In this experiment, the experimental data collection was completed by replacing the different faulty parts of the experimental wind turbine. In the experiment, the fault vibration waveform diagram is used as input data, and multiple locations in the wind turbine gearbox are collected separately, and the inner ring and outer ring of the gearbox, around the bearing, etc, are used for neural network training for 6 different vibration and electrical fluctuations, as shown in Figure 7. Show:

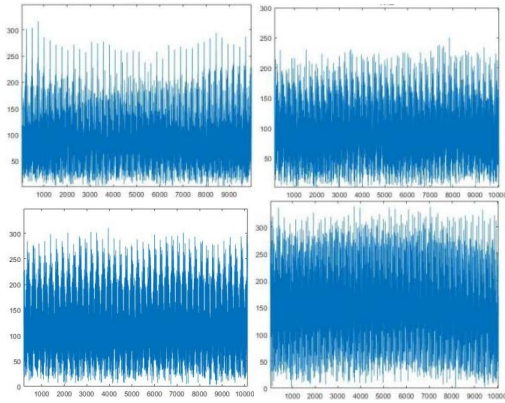


Figure 7. Vibration signal: a) tooth surface wear b) gear pitting c) gear broken tooth d) bearing failure

The vibration signal characteristics are in a non-linear distribution state, and there is no regularity between each sample data. The new sample data distribution state expanded by GAN is infinitely close to the original sample data distribution state, which verifies the validity of the wind turbine gear fault and bearing fault sample data generated by GAN, as shown in Figure 8.

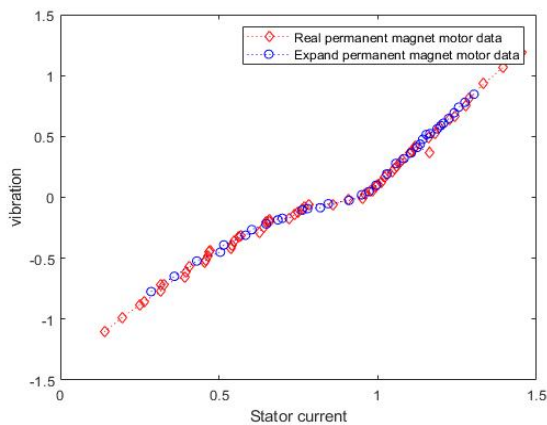


Figure 8. Training sample distribution

The loss rate of the diagnosis result of the generative adversarial neural network in training is 0%. Put the test samples into the trained neural network to judge the training results of wind turbine faults without error, and continuously upgrade and evolve through the generator and discriminator. The fluctuation of the training homeopathic rate was originally smaller and decreased, as shown in Figure 9.

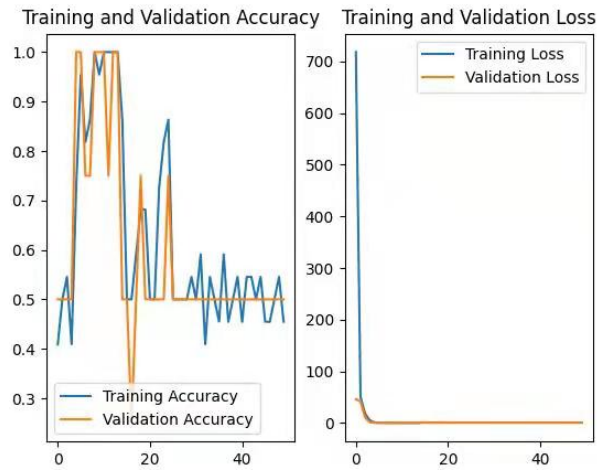


Figure 9. Network training accuracy and loss rate

4.3 Fault diagnosis of wind turbine gearbox based on DCGANN

The diagnostic model is modelled using a deep convolutional neural network, and the size of the data volume and the number of iterations will affect the accuracy of the model. According to the experimental results, it can be seen that the higher the number of iterations, the better the convergence of the diagnostic model, which also represents a better training effect of the neural network. The effectiveness of the diagnostic model is verified for 1000 groups of test samples, and the results show that the computational effect of the neural network reaches the optimum when the number of iterations is 100, and at this time, it is able to effectively diagnose the wind turbine gearbox faults.

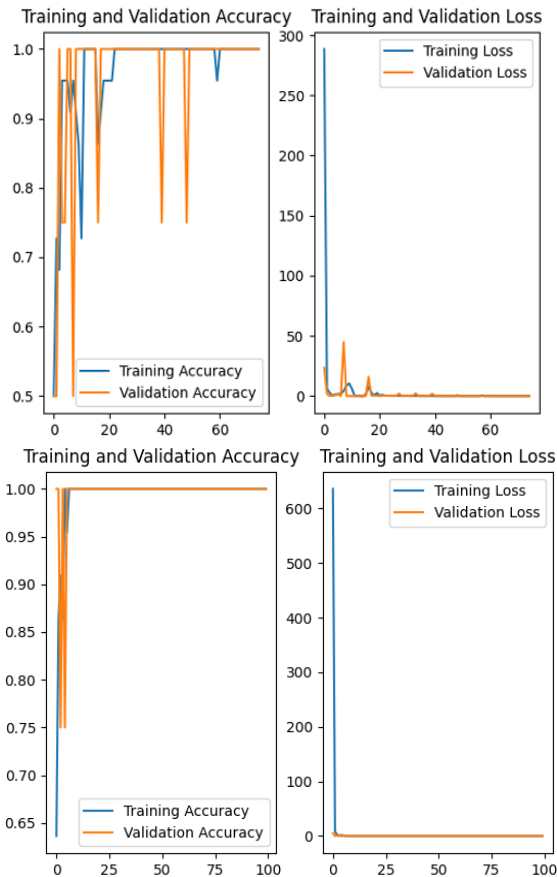


Figure 10. Network accuracy and loss rate of different iteration times

Assuming that all other conditions are the same except for the sample capacity, the accuracy of the neural network model gradually increases with the increase of the sample capacity. Through the extension of DCGAN, in order to meet the requirements of wind turbine gearbox fault diagnosis accuracy, the learning efficiency of the model can be improved by increasing the training set of the sample capacity, which provides a solution idea for the inefficiency in the process of solving the diagnosis problem using deep learning.

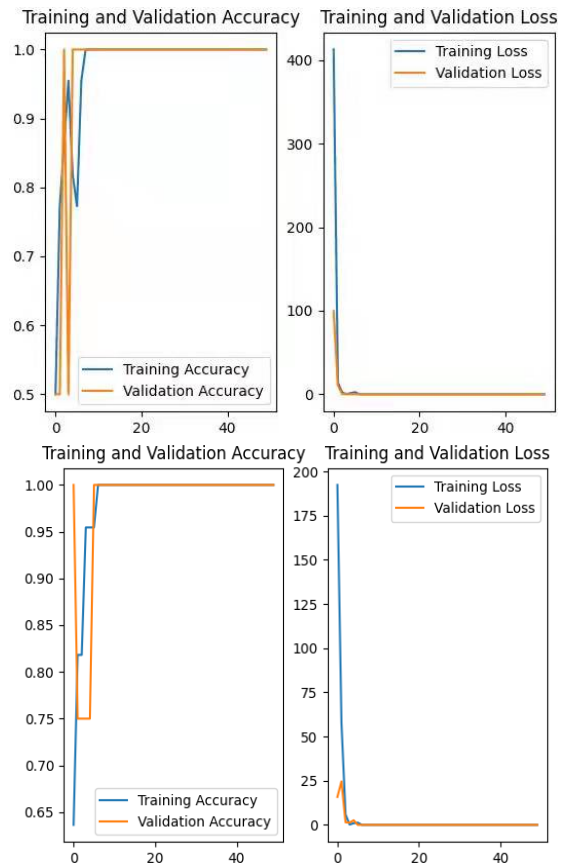


Figure 11. Sample network influence with trend items

As shown in the figure 10 and 11, through comparison, it can be found that after the trend item of vibration waveform data is decomposed by empirical mode after inputting the training data generated in the optimized deep convolutional neural network, it is better than the traditional generative formula. The accuracy of the training data generated by the adversarial neural network is much improved.

5. Conclusion

In this paper, a wind turbine gearbox fault diagnosis model based on EMD-DCGAN is proposed to address the problem of low diagnostic efficiency due to inaccurate data sources faced in wind turbine gearbox fault diagnosis. The model uses the signal processing mechanism of EMD to effectively eliminate the trend term of the vibration signal, and adopts the GAN deep neural network to classify the high-dimensional nonlinear vibration signal, so as to achieve the accurate identification of wind turbine gearbox faults. The specific conclusions are as follows:

- (1) Use EMD to improve data accuracy and solve the problem that the vibration signal is affected by the trend item, and the vibration acceleration signal will deviate from the baseline. The signal processing mechanism of EMD can effectively eliminate the trend term of the

vibration signal, and make the sample data more suitable for the training of the diagnostic model, improve the training accuracy and speed of the diagnostic model, and provide a data basis for the diagnosis of wind turbine gearbox faults..

(2) Using DCGAN to construct a fault diagnosis model to monitor the wind turbine gearbox, optimize the network structure and adjust the parameters to improve the accuracy of network training. The experimental results show that EMD-DCGAN can solve the problem of insufficient training samples and can significantly strengthen the training of the network Ability, fault diagnosis accuracy rate has obvious advantages over other neural networks.

Acknowledgements.

This work was supported by the Innovation Capability Enhancement Joint Fund of Liaoning Province Department of Science and Technology, China (2022-NLTS-16-03).

References

- [1] Zhou Z. Review of fault diagnosis technology of fan gearbox [J]. *Technology and Market*, 2016,23 (04): 25-26+28.
- [2] Ma Weiwei. Current situation and development trend of international wind power industry [J]. *Enterprise Reform and Management*, 2019 (15): 209-213.
- [3] Qiao L. Current situation and prospect of global wind power development [J]. *Wind Energy*, 2012 (09): 58-62.
- [4] Xia Yunfeng. Inventory of China's wind power policy in 2019 [J]. *Wind Energy*, 2020 (01): 64-70.
- [5] Li Haozhang, Liu Pingyuan, Wang Jinhong, et al. Analysis of the present situation and future prospect of China's wind power industry [J]. *Electromechanical Information*, 2020 (21): 91-94.
- [6] Ji Z. Research on the present situation and development trend of wind power industry in China [J]. *china plant engineering*, 2020 (18): 217-218.
- [7] Qin Haiyan. The wind power industry will achieve high-quality development in 2018 [J]. *Wind Energy*, 2018 (12): 1-1.
- [8] Information Office of the State Council of the People's Republic of China. China's energy development in the new era [N]. *People's Daily*, 2020-12-22(010).
- [9] Miao He, David He. Deep Learning Based Approach for Bearing Fault Diagnosis[J]. *IEEE Transactions on Industry Applications*, 2017, 53(3): 3057-3065.
- [10] Fu C. Research on fault diagnosis method of fan gearbox based on deep learning [D]. *Jiangnan University*, 2020.
- [11] Wang Qingzhao, Wang Mingjun, Zhu Bin. Analysis of major accidents of wind turbines (I) [J]. *Wind Energy*, 2014 (06): 60-63.
- [12] Zhang P, Lu D. A survey of condition monitoring and fault diagnosis toward integrated O&M for wind turbines[J]. *Energies*, 2019, 12(14): 2801.
- [13] de Azevedo H D M, Araújo A M, Bouchonneau N. A review of wind turbine bearing condition monitoring: State of the art and challenges[J]. *Renewable and Sustainable Energy Reviews*, 2016, 56: 368-379.
- [14] Chen X, Guo Y, Xu C, et al. Review of research on fault diagnosis and health monitoring of wind power equipment [J]. *China Mechanical Engineering*, 2020,31 (02): 175-189.
- [15] Li H, Xiao D. Overview of data-driven fault diagnosis methods [J]. *Control and Decision*, 2011,26 (1): 1-9+16.
- [16] Menezes E J N, Araújo A M, da Silva N S B. A review on wind turbine control and its associated methods[J]. *Journal of cleaner production*, 2018, 174(6): 945-953.
- [17] CHEN J, LIU Z, WANG H, et al. Automatic defect detection of fasteners on the catenary support device using deep convolutional neural network[J]. *IEEE Transactions on Instrumentation and Measurement*, 2017, 67(2): 257-269.
- [18] Zhang Wei, Bai Kai, Song Peng, et al. Fault feature extraction method of fan rolling bearing based on VMD and singular value energy difference spectrum [J]. *North China Electric Power Technology*, 2017 (3): 59-64.
- [19] ZHAO S, YIN L, ZHANG J, et al. Real-time fabric defect detection based on multi-scale convolutional neural network[J]. *IET Collaborative Intelligent Manufacturing*, 2020, 2(4): 189-196.
- [20] REDMON J, DIVVALA S, GIRSHICK R, et al. You only look once: unified, real-time object detection[C]. *IEEE Conference on Computer Vision and Pattern Recognition*, Las Vegas: IEEE, 2016:779-788.